European Journal of Cell Biology 98 (2019) 151044

Contents lists available at ScienceDirect

European Journal of Cell Biology

journal homepage: www.elsevier.com/locate/ejcb

Research paper

Cripto-1 localizes to dynamic and shed filopodia associated with cellular migration in glioblastoma cells

Johann Mar Gudbergsson*, Meg Duroux*

Laboratory of Immunology and Cancer Biology, Department of Health Science and Technology, Faculty of Medicine, Aalborg University, Fredrik Bajers Vej 3B, 9220 Aalborg Ø, Denmark

ARTICLE INFO

Keywords:
Cripto-1
CD44
Subcellular
Dynamics
Filopodia
Vesicles
EV
Secretion
In vitro
Glioblastoma
Retraction fibers
Tunneling nanotubes

ABSTRACT

Cripto-1 is a protein participating in tissue orientation during embryogenesis but has also been implicated in a wide variety of cancers, such as colon, lung and breast cancer. Cripto-1 plays a role in the regulation of different pathways, including TGF-β/Smad and Wnt/β-catenin, which are highly associated with cell migration both during embryonal development and cancer progression. Little is known about the detailed subcellular localization of cripto-1 and how it participates in the directional movement of cells. In this study, the subcellular localization of cripto-1 in glioblastoma cells was investigated *in vitro* with high-resolution microscopy techniques. Cripto-1 was found to be localized to dynamic and shed filopodia and transported between cells through tunneling nanotubes. Our results connect the refined subcellular localization of cripto-1 to its functions in cellular orientation and migration.

1. Introduction

Cripto-1 protein (TDGF1 gene) is a member of the evolutionarily conserved epidermal growth factor-Cripto-1/FRL/Cryptic (EGF-CFC) family, and is a co-receptor in several stemness-associated pathways such as the TGF-β/Smad and Wnt/β-catenin pathways (Bianco et al., 2010; Ravisankar et al., 2011; Strizzi et al., 2005). Both of these pathways are highly involved in embryonic development, making cripto-1 a co-regulator of embryogenesis (Warner et al., 2005). More specifically, cripto-1 has been shown to become expressed during gastrulation in a polarized pattern, essential for orientation of the anterior-posterior axis during embryonic development acting as a co-receptor for Nodal (Beck et al., 2002; Ding et al., 1998). Cripto-1 was also crucial for the formation of foregut endoderm, prechordal mesoderm and the notochordal plate, and it was shown that cripto-1 could exogenously exert these effects (Chu et al., 2005). Since most types of cancer harbor subpopulations of cells with stem cell properties, re-expression of cripto-1 has been discovered in several tumor types (Francescangeli et al., 2015; Klauzinska et al., 2014; Liu et al., 2017a, b; Pilgaard et al., 2014; Strizzi et al., 2013, 2005; Tysnes et al., 2013). Cellular processes such as epithelial-mesenchymal transition (EMT), invasion and treatment resistance have been associated with cripto-1 expression (Huang et al., 2015; Normanno et al., 2004; Strizzi et al., 2004).

In line with cripto-1 being associated with cellular invasiveness, cripto-1 was also localized to migrating cells in extravillous trophoblast in abnormal percreta placenta samples (Bandeira et al., 2014). The mechanisms of cell migration in healthy and disease-related processes rely on distinctive subcellular structures, including cellular protrusions such as lamellipodia and filopodia. Lamellipodia are the largest of cellular projections and filopodia are small protrusions typically formed at the leading edge from lamellipodia (Jacquemet et al., 2015; Yang and Svitkina, 2011). Filopodia have been shown to play a key role in cell adhesion and sensing the surrounding environment, directing cellular migration during embryonal development and tissue patterning (Sanders et al., 2013; Stanganello et al., 2015; Steketee and Tosney, 2002). In ways similar to healthy cells, cancer cells use cellular protrusions such as filopodia to invade surrounding tissue and metastasize to distant sites (Arjonen et al., 2011; Jacquemet et al., 2015; Machesky, 2008).

Cripto-1 has become a popular prognostic biomarker in an array of cancer types and shown to have a number of very different functions (Jain et al., 2018; Pilgaard et al., 2014; Wei et al., 2015; Xu et al., 2017; Zhang et al., 2018). However, not much is known about its detailed subcellular localization in glioblastoma. In this study, we set out to

* Corresponding authors.
E-mail addresses: jmg@hst.aau.dk (J.M. Gudbergsson), megd@hst.aau.dk (M. Duroux).

https://doi.org/10.1016/j.ejcb.2019.151044
Received 23 May 2019; Received in revised form 22 July 2019; Accepted 24 July 2019

explore the dynamics of cripto-1 localization with respect to distinct subcellular structures that are linked to its reported function in the literature. Interestingly, we discovered cripto-1 was highly expressed in tunneling nanotubes, dynamic filopodia and shed filopodia/retraction fibers. This novel finding, to the best of our knowledge, has not been previously been reported for cripto-1 and could highlight an important role for this protein in mitigating cell migration and invasion in GBM.

2. Materials and methods

2.1. Cell culture

U87MG cells were grown with Gibco DMEM-F12 with Glutamax (Thermo Scientific; #10565018) supplemented with 10% Fetal Calf Serum (FCS) and 1% penicillin-streptomycin. Detachment of cells during passaging was done with trypsin/EDTA.

2.2. Stable transfection

U87MG cells were transfected with Lipofectamine 2000 (Thermo Scientific; #11668027) using the wet-reverse approach (Rasmussen et al., 2016). Briefly, 1 μg of plasmid DNA was mixed with lipid reagent and DMEM medium and spread across the bottoms in a 6 well plate. U87MG cells were then seeded on top of the lipid-DNA mixture for transfection. After 48 h, selection pressure with G418 (Sigma; #A1720-1 G; 400 μg/mL) was applied for 10 days or until all empty vector controls were dead. Selection pressure was maintained with a half dose of G418 (200 μg/mL). To generate empty vector controls, cripto-1 sequence was cut out with restriction enzymes and purified with GeneJET Gel Extraction Kit (Thermo Scientific; #K0691) and concentration measured with NanoDrop 2000 (Thermo Scientific). Cells were then stably transfected with the empty vector as described above. Cripto-1 plasmid was kindly provided by Dr. David S. Salomon (Normanno et al., 2004).

2.3. Western blot

Cells were lysed with RIPA buffer on ice and the lysate was subsequently centrifuged at 10.000 RCF for 10 min to clear cell debris and large aggregates. Protein concentration was measured at A280 on NanoDrop 2000 (Thermo Scientific). Lysates were then mixed with Laemmli buffer (1x) and boiled for 5 min. Precast Mini-PROTEAN 4–20 % SDS-PAGE gels (BioRad; #4561094) were loaded with 100 μg, 50 μg and 20 μg of protein from transfected and empty vector U87MG lysates and run for 40 min. Blotting was done with Trans-Blot Turbo Transfer System (Bio-Rad, #1704150) onto a nitrocellulose membrane using the Mini-PROTEAN TGX protocol. Membrane was blocked with 5% skimmed milk in TBS, washed, and stained with primary antibodies (see Table S1) overnight at 4 °C on an orbital shaker. Membrane was washed and incubated with secondary antibodies (Table S1) for 2 h at RT on an orbital shaker.

2.4. Flow cytometry

Cells were dissociated with sodium citrate buffer (1.35 M KCl, 0.15 M sodium citrate in dd water) for 5 min at 37 °C. The culture flask was gently tapped to loosen cells and cells were resuspended in 1:1 PBS and centrifuged at 300 RCF. Cells ($\sim 1 \times 10^6$) were stained with Ms-anti-cripto-1-PE antibody (R&D Systems; #FABP2772; 1:500, Table S1) in ice cold PBS with 3% BSA for 30 min. at 4 °C. Stained cells were washed three times in PBS and resuspended in PBS with 10% FCS and immediately analyzed by flow cytometry (CytoFLEX S; Beckman Coulter). Both empty vector and no-stain controls were included. Data was analyzed and visualized with Kaluza Analysis software (Beckman Coulter).

2.5. Immunocytochemistry

Cells were grown on coverslips and fixed by adding 4% formaldehyde 1:1 to the well for pre-fixation for 5 min. and then postfixed in 4% formaldehyde for another 10 min. Cells were washed and blocked with 5% BSA in PBS for 1 h at RT and stained with primary antibodies (see Table S1) overnight at 4 °C on an orbital shaker. Cells were then washed and stained with secondary antibodies (Table S1) for 2 h at RT on an orbital shaker. Nuclear stain (Hoechst33342; Thermo Scientific; #62249; 1:3000) was added during the last 15 min. of secondary antibody incubation. Coverslips were mounted on SuperFrost Plus slides (Thermo Scientific; #J1800AMNZ) with Fluorescent Mounting Media (DAKO/Agilent; #S3023). Slides were stored in the dark at 4 °C overnight to let mounting medium harden. Images were acquired on a Zeiss Observer Z.1 with Apotome.2. Apotome focus calibration was done and apotome settings were set to take 5 images per Z plane. Z-stacks were acquired through the whole cellular layer and Z-stack projection was done with maximum intensity settings using Fiji (Schindelin et al., 2012).

2.6. Scanning electron microscopy

U87MG were seeded onto silicium slides and fixed by 2% formaldehyde and 2% glutaraldehyde in PBS for 30 min. at RT. Cells were washed and subsequently dehydrated in a series of ethanol concentrations (50%, 60%, 70%, 80%, 90% and 100%) each for 10 min. Samples were then dried and Au-coated before imaging with a Zeiss EVO 60 scanning electron microscope at 8 kV.

2.7. Live-cell spinning disk confocal imaging

U87MG cells were grown on coverslips and stained with CellMask Deep Red (Thermo Scientific; #C10046; 1:1000) in growth medium for 10 min. at 37 °C. Cells were washed and mounted in the confocal chamber with growth medium containing residual dye. Imaging was performed with a Zeiss Observer Z.1 mounted with a motorized stage and live cell incubator with temperature, gas and humidity control. The microscope was equipped with a spinning disk confocal system (CSU-X1; Yokogawa) and Ixon3 EMCCD camera (Andor) for live-cell acquisition. Acquisition was done using Colibri LED illumination and an alpha Plan-apochromat 100x/1.46NA oil objective (Zeiss). Exposure time was 60 ms and time series were done with 2–10 s between frames.

3. Results

3.1. Cripto-1 localizes to tunneling nanotubes and filopodia

Induced expression of cripto-1 was verified with western blot and flow cytometry which showed approximately 20% of cells stably expressing cripto-1 (Fig. 1 A–B). Since cripto-1 has been implicated in tissue organization and orientation during embryogenesis (Ding et al., 1998), we hypothesized that cripto-1 could be localized to invadopodia and filopodia. Here, we defined invadopodial puncta as small cell protrusions containing both cortactin and F-actin as shown in Fig. 1C. However, cripto-1 did not colocalize with Cortactin in invadopodial puncta (Fig. 1D). Instead, it was observed that cripto-1 was present in tunneling nanotubes, seemingly transported between cells (Fig. 2A), and highly expressed in filopodia which seemed to be shed from the cells at the trailing edge resembling a cellular “snail trail” (Fig. 2B). With scanning electron microscopy, both tunneling nanotubes (yellow arrow) and filopodia could be visualized. Filopodia were extending from a lamellipodium (white arrows), confirming these structures contained plasma membrane (Fig. 2C).

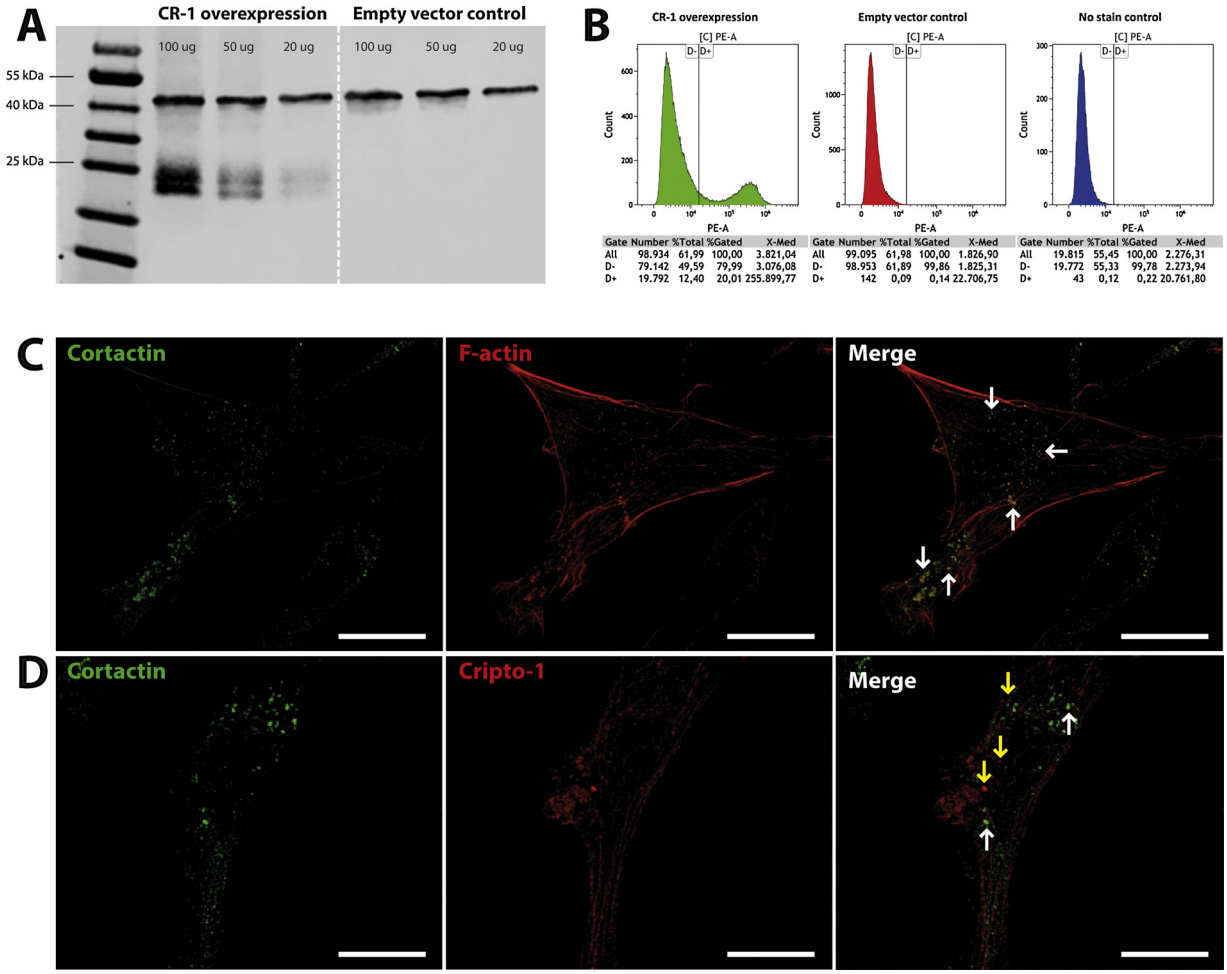

Fig. 1. A) Western blot of lysates from cripto-1 overexpressing cells. Cripto-1 is present in the overexpressing cells and shows a band under 25 kDa. B) Flow cytometry of cripto-1 overexpressing cells showing around 20% stably transfected. C) Cortactin and F-actin co-localization in invadopodial puncta (white arrows). D) Cortactin and cripto-1 co-staining showing no co-localization. White arrows indicate cortactin, yellow indicate cripto-1. Scale bars = 10 μm. (For interpretation of the references to colour in this figure legend, the reader is referred to the web version of this article).

3.2. Cripto-1 and CD44 colocalize in shed cellular fragments

We consistently observed cripto-1-positive shed fragments close to cripto-1 overexpressing cells (Fig. 3A). We hypothesized that these structures could be involved in the cellular interaction with extracellular matrix (ECM) and were left behind during cell movement. With regard to this interesting observation, we wanted to see if the shed fragments were a result of cripto-1 expression. Cripto-1 overexpressing cells were co-stained with cripto-1 and CD44 and we discovered that CD44 was located to these fragments (Fig. 3B, white arrows). Here, we observed that both CD44 + cripto-1 and CD44-only fragments were present, and hence we could distinguish the fragments from cripto-1 overexpressing and non-expressing cells (Fig. 3B, yellow arrows).

Using live-cell spinning disk confocal imaging, we determined the nature of the shed fragments by examining their dynamics in U87MG cells stained with the lipophilic membrane stain CellMask Deep Red. The fragments were easily identified and present to a varying extent attached to or around all cells. We managed to capture images of cells actively making the cell fragments and observed that lamellipodia-like structures of the cells were retracted within a few seconds and in that process, membrane-derived fragments were left behind attached to adhesion spots (Fig. 4A, Video S1). Interestingly, smaller filopodia-like cell protrusions were left behind cell-derived fragments after retraction of the protrusion (Fig. 4B, Video S2).

3.3. Cripto-1 localizes to dynamic filopodia

On several occasions, the transfer of cripto-1-positive vesicle-like structures to cripto-1 negative cells *via* tunneling nanotubes was observed (Fig. 5A). Similarly, we captured images of cripto-1-positive vesicle-like structures attached to the cell membrane in what appeared to be a process like cellular expulsion of these vesicles (Fig. 5B). In addition, cripto-1 was present in similar vesicle-like structures with a longer membrane actin-based attachment, resembling cripto-1 rosebuds on an actin stalk (Fig. 5C). Thus, we hypothesized that cripto-1 could be incorporated into cell-derived vesicles such as exosomes or microvesicles. The most widely used marker for exosomes and multivesicular bodies (in which exosomes are formed) is CD63. Therefore, we did a co-staining of cripto-1 and CD63. Cripto-1 did not appear to localize to the same intracellular structures as CD63, hence excluding packaging into exosomes, leaving us to believe it was microvesicle-based secretion (Fig. 5D). However, looking at live-cell imaging, it became apparent that these structures weren't extracellular vesicles, but rather attached to the cells in what appeared to be two different structures (Fig. 6, Video S3–6). One structure resembled the longer structures observed in Fig. 5C, which were attached to the cell membrane resembling highly dynamic filopodia, moving rapidly in all dimensions (Fig. 6A–C white arrows, Video S3–5). The other structure looked like a temporary bulging of the plasma membrane, also happening within a few seconds (Fig. 6C-D yellow arrows, Video S5-6). Contrary to shed filopodia, the

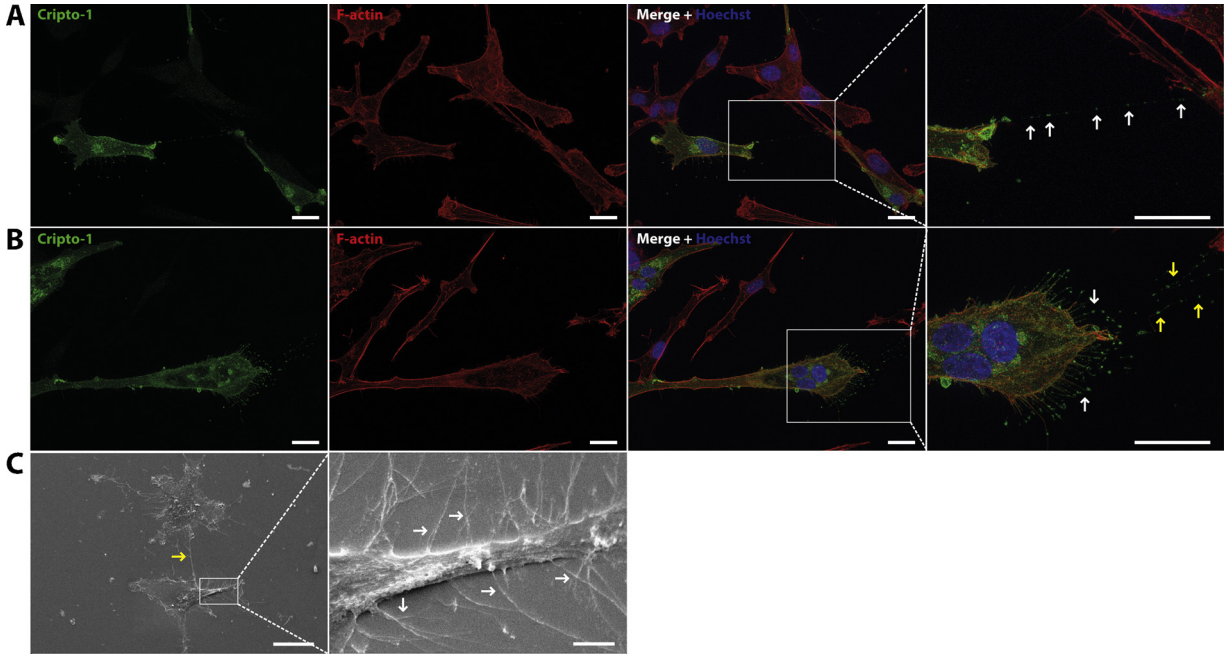

Fig. 2. Cripto-1 in tunneling nanotubes and filopodia. A) Cripto-1 and F-actin co-staining showing cripto-1 transfer from cripto-1 overexpressing cell to cripto-1 negative cell *via* tunneling nanotube. White arrows indicate cripto-1-positive focal points along a tunneling nanotube between two cells. Scale bars = 20 µm. B) Multinuclear cripto-1 overexpressing cell with cripto-1 positive filopodia extending from the trailing edge. White arrows point to cripto-1-positive filopodia attached to the cell. Yellow arrows indicate cripto-1-positive focal points shed from the trailing edge. Scale bars = 20 µm. C) Scanning electron micrographs of tunneling nanotube and filopodia extending from a cellular lamellipodium. Scale bars in picture 1 = 10 µm and in zoom-in = 2 µm. (For interpretation of the references to colour in this figure legend, the reader is referred to the web version of this article).

dynamic structures were easier to visualize when the focal plane of the confocal microscope was above the bottom of the culture dish, to enable visualization of cellular structures that were not in contact with the surface of the dish. As captured in the videos, both structures were highly active during cytokinesis, the last stage of cell division. The dynamic filopodia were also highly present in larger cellular protrusions. It could be shown that these structures could interact with the shed filopodia / retraction fibers, as illustrated by dynamic filopodia protruding from a lamellipodia pulling strings from shed, static filopodia (Fig. 7, Video S7-8).

4. Discussion

Cripto-1 has a broad portfolio of cellular functions both in health and disease and has been investigated extensively in relation to cancer. The involvement of cripto-1 in the facilitation of tumor progression, and the distribution within malignant cells with respect to cellular localization would shed light on some the reported functions. In this study, we mapped the subcellular localization of cripto-1 by structured illumination microscopy in U87MG cells overexpressing cripto-1 *in vitro* and investigated the dynamics of the cripto-1-enriched structures by live-cell confocal microscopy.

Cripto-1 was found to be expressed in tunneling nanotubes and filopodia with highest signal intensity at the filopodia tip as a round cripto-1-positive 'spot'. Filopodia have previously been characterized in cultured U87MG and other glioblastoma cells by scanning electron microscopy, cementing the importance of these structures *in vitro* (Albuschies and Vogel, 2013; Memmel et al., 2014). *In vivo*, filopodia

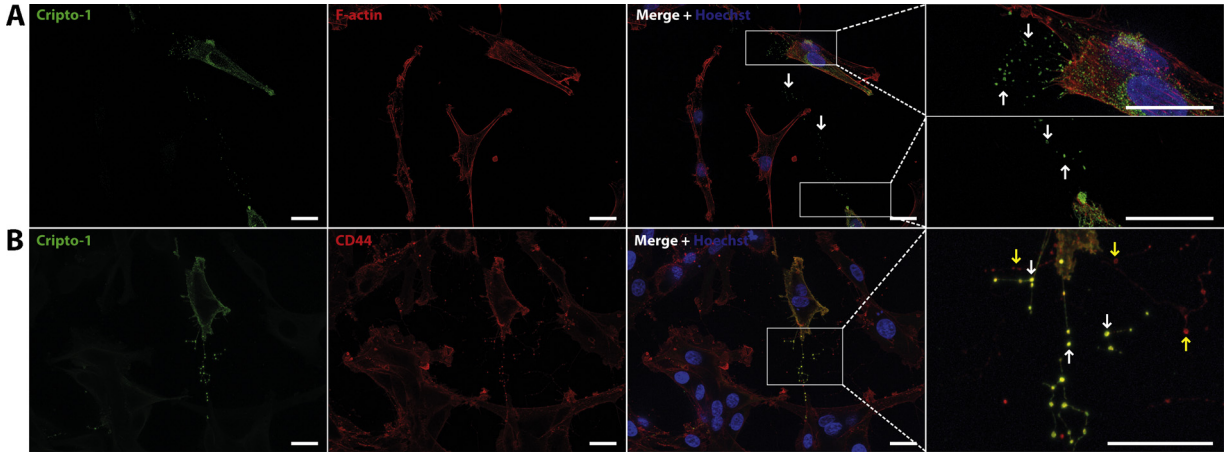

Fig. 3. Cripto-1 positive filopodia shed from trailing edge. A) Cripto-1 in shed filopodia from the trailing edge (white arrows). B) Cripto-1 and CD44 co-localize in shed filopodia from cripto-1 overexpressing cells (white arrows). Yellow arrows point to CD44-positive/Cripto-1-negative shed filopodia. Scale bars = 20 µm. (For interpretation of the references to colour in this figure legend, the reader is referred to the web version of this article).

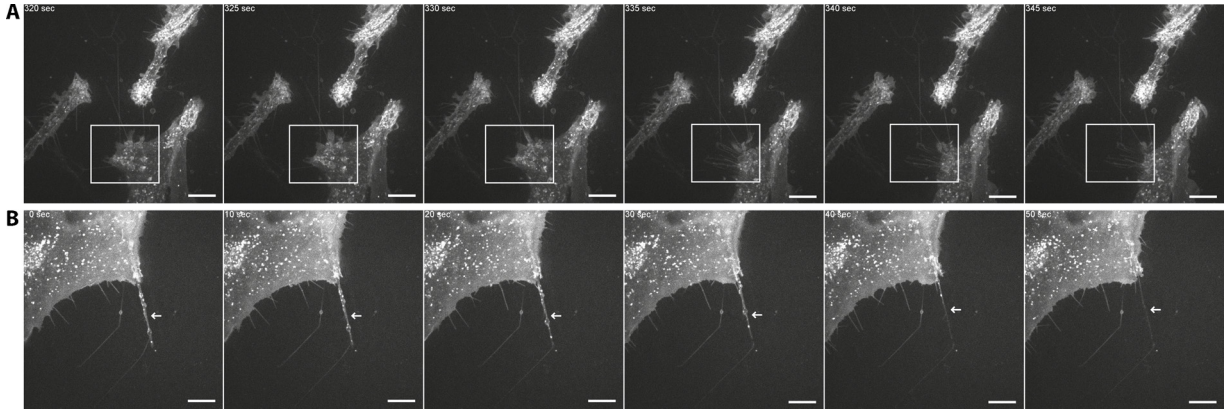

Fig. 4. Live cell imaging of shed filopodia / retraction fibers. A) Retraction of a lamellipodium leaves membranous structures behind (white box). B) Retraction of filopodium leaves membranous structure behind (white arrow). Scale bars = 10 µm.

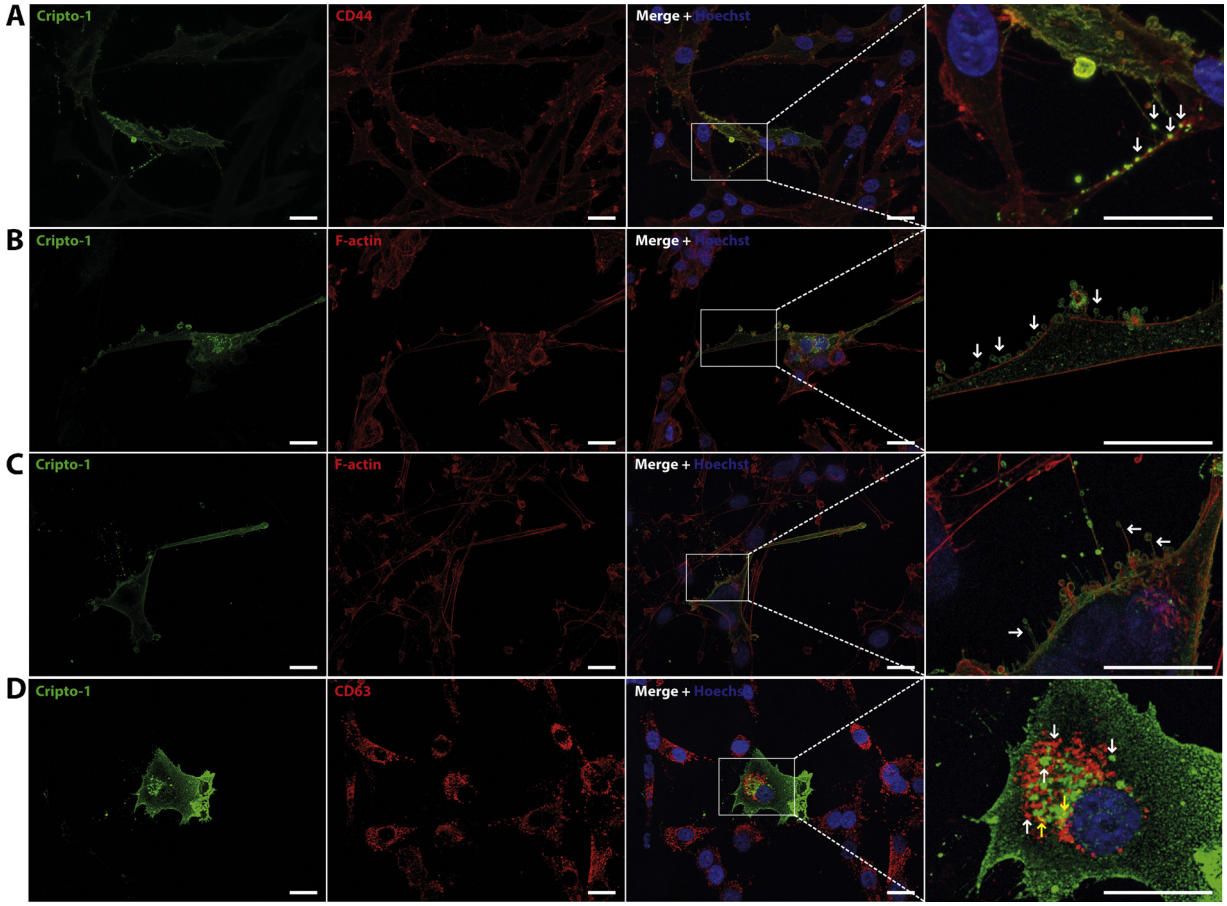

Fig. 5. Vesiculation of cripto-1. A) Transfer of cripto-1 positive vesicle-like structures *via* tunneling nanotubes. B) Donut-shaped cripto-1 positive vesicle sprouting from the plasma membrane. C) Actin-rich filopodia with donut-shaped cripto-1 positive vesicle-like structures at the tip. D) Cripto-1 and CD63 do not localize to the same intracellular vesicles. White arrows indicate cripto-1-positive structures. Yellow arrows indicate CD63 and cripto-1 co-localization, most likely an artifact of Z-stack projection. Scale bars = 20 µm. (For interpretation of the references to colour in this figure legend, the reader is referred to the web version of this article).

play a role in cellular communication, sensing the surrounding environment for directional migration during angiogenesis and cancer cell migration and invasion (Arjonen et al., 2011; Fantin et al., 2015; Sagar et al., 2015). Here, we observed that the cells shed cripto-1 and CD44-positive fragments from the trailing edge that seemed to be derived from the trailing edge filopodia. Live-cell confocal imaging with lipophilic dye showed that these shed structures also retained the dye, an indication that the plasma membrane was still intact. A study published in 2004, observed and discussed a highly similar process with CD44 and Integrin β1-positive cell fragments shed from the trailing edge of melanoma cells embedded in a collagen matrix *in vitro* (Mayer et al., 2004). They reported that this process was Integrin β1-dependent and suggested that this represents a fundamental mechanism for cell detachment from adhesive substrates (Mayer et al., 2004). Endoglin (CD105) and CD31 were observed in similar structures in endothelial cells during vascular sprouting in samples from human fetal telencephalon, indicative of this not being limited to cultured cells *in vitro* but also present *in vivo* (Virgintino et al., 2012). These structures resemble what is termed 'retraction fibers' in other studies, which were first described in 1945 (Porter et al., 1945). To date, while not many

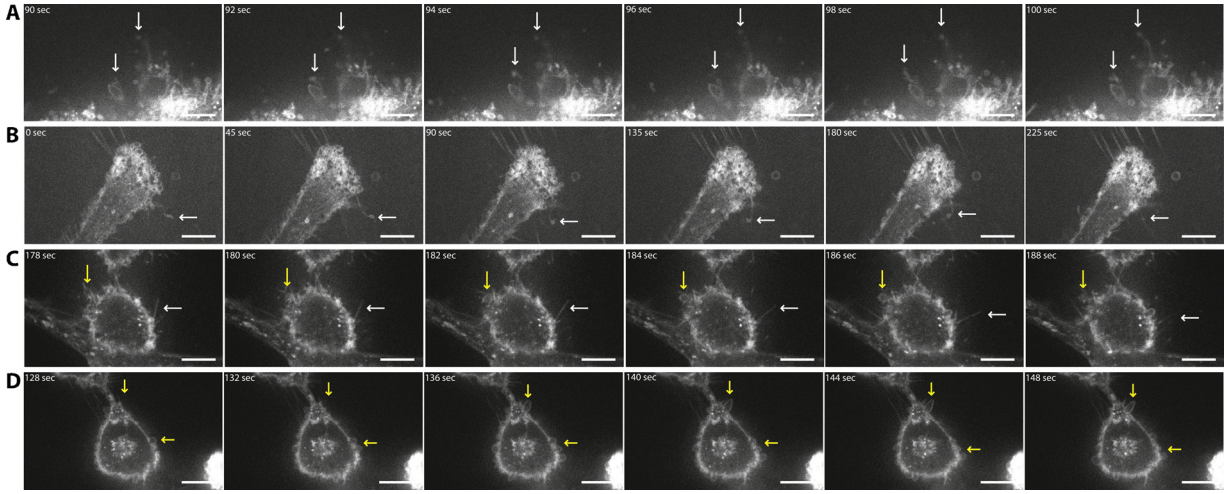

Fig. 6. Live cell imaging of dynamic cellular protrusions. A) Highly dynamic filopodia structures (white arrows) visible at a focal plane in the middle/top of the cell (Video S3). B) Dynamic filopodia reaching in all directions (white arrow) while larger lamellipodia interacts with shed filopodia/retraction fibers from another cell (Video S4). C) Dynamic filopodia (white arrows) and membrane bulging (yellow arrows) in a cell in the final stages of cytokinesis. Focal plane at the bottom at cell-dish interface. (Video S5). D) Same cells undergoing cytokinesis with the focal plane in the middle of the cell. Membrane bulging shown in yellow arrows (Video S6). Scale bars = 10 µm. (For interpretation of the references to colour in this figure legend, the reader is referred to the web version of this article).

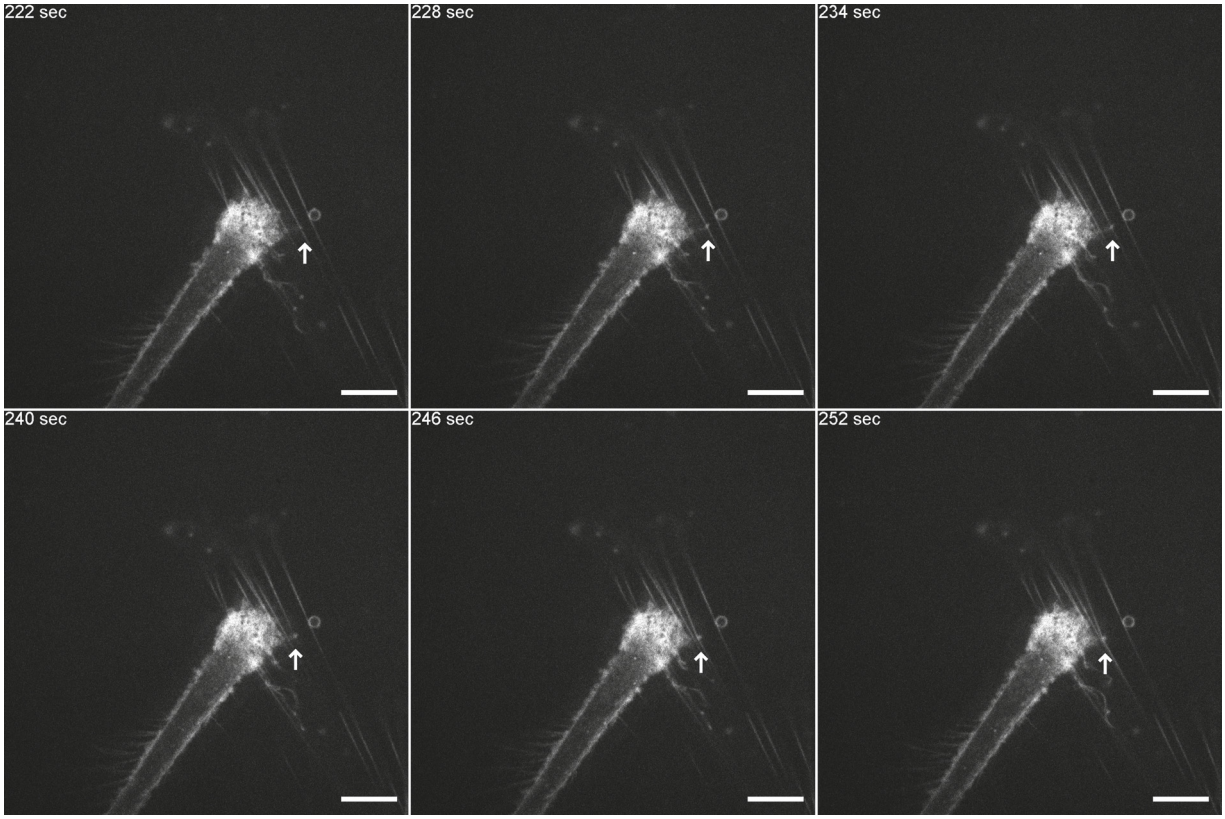

Fig. 7. Dynamic filopodia pulling the shed filopodia/retraction fibers from another cell (white arrow, Video S7). Scale bars = 10 µm.

studies have been published on these structures, a few have investigated retraction fibers and the structures in the studies look highly similar to what we have observed (Amieva and Furthmayr, 1995; Cramer and Mitchison, 1997; Ma et al., 2015; Mitchison, 1992; Taylor and Robbins, 1963). One paper studying microspikes, filopodia and retraction fiber dynamics, suggested that these structures are the same just pictured at different points in time, and thus collectively referred to them as filopodia (Svitkina et al., 2003). In relation to these cellular protrusions, a study noticed microvesicle-like structures, which they believed to be shed from the cells, much resembling our own observations reported here (Virgintino et al., 2012). Similarly, CD44-positive vesicle-like structures were reported to be shed from filopodia in gastric carcinoma cells *in vitro* and *in vivo* (Härkönen et al., 2019). However, we observed in our fluorescence images that most of these vesicle-like structures were attached to actin-fibers, and live-cell imaging confirmed that these structures were indeed dynamic protrusions of the plasma membrane or static cell-derived fragments/retraction fibers. Instead of being shedding microvesicles, this could indicate that the structures observed could in fact be filopodia. This is supported by a study conducted by Ma et al. who characterized these shed cellular

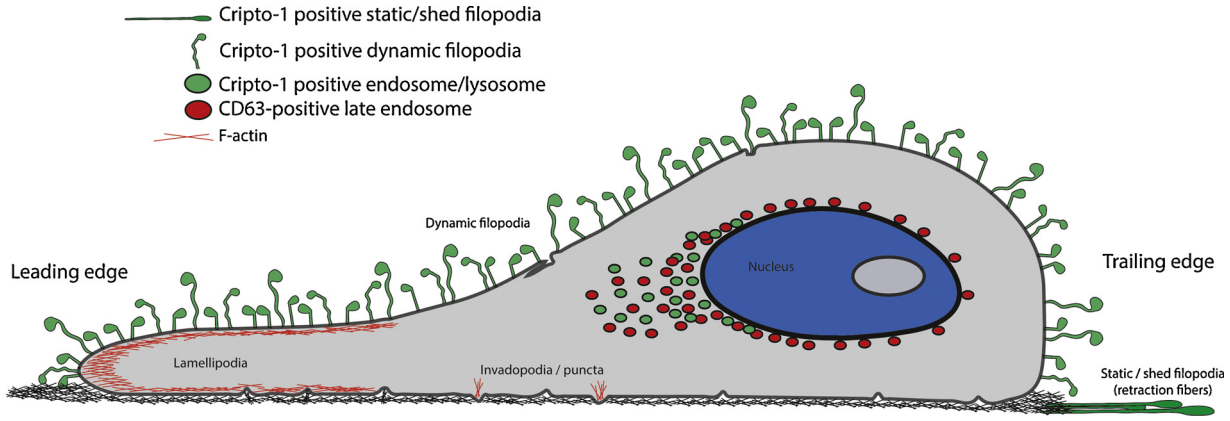

Fig. 8. Illustration of cripto-1-positive structures found in this study.

fragments ultrastructurally, and found that they are indeed long membrane-derived filopodia-like fragments (or retraction fibers) which may contain intracellular vesicles (Ma et al., 2015). In search of what others have reported on similar vesicle- or spot-like patterns, we came across a few studies showing similar structural distribution (Almagro et al., 2010; He et al., 2017; Watanabe et al., 2010). These studies all reported that myosin-X contributes to filopodia formation through multiple elongation cycles, and orchestrates in a phenomenon known as 'myosin-X spots' which are highly similar to the vesicle-like structures and the shed cell fragments reported in this study and others (Almagro et al., 2010; He et al., 2017; Watanabe et al., 2010). Since filopodia are formed through multiple elongation cycles and at each point of elongation a myosin-X spot is formed, we hypothesize that these myosin-X spots and the cripto-1 positive spots observed here could be focal adhesion spots that at some point might be "left behind" or shed from the cells dependent on the cells' decision on the direction of migration (Jacquemet et al., 2015). This is supported by myosin-X playing a crucial role in transport of Integrin β1 to filopodia and the presence of Integrin β1 in the shed filopodia-like structures (Arjonen et al., 2011; Mayer et al., 2004; Zhang et al., 2004). Furthermore, focal adhesion spots have been shown ultrastructurally to be arranged in round, hollow structures (Patla et al., 2010). Hence, all cripto-1-positive structures observed in this study seem to be affiliated with filopodia, filopodia-based focal adhesion and shed filopodia / retraction fibers. Cripto-1 has been observed to elicit paracrine and autocrine functions by being cleaved from the plasma membrane by phospholipase D (Watanabe et al., 2007; Watanabe and Salomon, 2010). The results presented in this study could represent an additional mechanism of paracrine cripto-1 signaling by shedding cripto-1-positive filopodia for surrounding cells to interact with.

Cripto-1 has been associated with the dynamic regulation of stemness in cancer as a co-receptor in the Wnt/β-catenin and TGF-β1/Activin receptor pathways which are highly associated with epithelial-mesenchymal transition (EMT) and cancer cell invasion and migration (Francescangeli et al., 2015; Liu et al., 2017b; Lo et al., 2018). Moreover, cripto-1 has also been shown to be required for correct tissue orientation of the anterior-posterior axis in the mouse embryo (Ding et al., 1998), rationalizing the subcellular distribution of cripto-1 to filopodia since morphogen transport during embryonal development has been shown to be done *via* filopodia (Fairchild and Barna, 2014). In line with this, Wnt proteins have been shown to localize to filopodia *in vitro* and *in vivo* in a spot-like fashion similar to what we have described here (Luz et al., 2014; Mattes et al., 2018; Moti et al., 2019). One study even showed that Wnt8a colocalized with myosin-X in filopodia in a zebrafish embryo *in vivo* (Stanganello et al., 2015). This all substantiates our findings of cripto-1 localization to filopodia. In summary, we have illustrated our findings on how cripto-1 subcellular localization looks within a migrating cancer cell in 2D cell culture (Fig. 8). We propose that the abundance of highly dynamic filopodia in culture is restricted to 2D culturing, as we would expect them to interact with other cells or ECM in the event of a 3D setting and thus become less dynamic and less abundant due to higher turnover. In future experiments, the cripto-1 field of research would benefit from an examination of the wildtype nature of cripto-1 in GBM using more clinically relevant GBM cell models and complex 3D setups *in vitro* supported with *in vivo* GBM xenograft experiments (Gudbergsson et al., 2019).

5. Conclusion

In conclusion, we have mapped cripto-1 protein to distinct subcellular structures related to cellular migration, namely filopodia, which has not been previously reported in any type of cell. Cripto-1 was present in dynamic filopodia, focal adhesion-like spots in filopodia and in shed filopodia, all involved in different stages of cellular migration. We thus conclude that the subcellular localization of cripto-1 fits well with the reported functions of migration of cells in health and disease.

Declaration of Competing Interest

The authors declare no conflict of interest.

Acknowledgements

The authors would like to thank Professor Torben Moos at Aalborg University for providing excellent facilities for structured illumination microscopy, and Core Facility for Integrated Microscopy (CFIM) at University of Copenhagen for facilitating live-cell spinning disk confocal microscopy. Furthermore, we would like to thank Zdeněk Plšek for assistance with western blotting. Lastly, we thank Christian B. Stolberg, Nichlas Karred and the Department for Physics and Nanotechnology at Aalborg University for assisting with scanning electron microscopy. This study was partially funded by Augustinus Fonden (application#15-5052).

Appendix A. Supplementary data

Supplementary material related to this article can be found, in the online version, at doi:https://doi.org/10.1016/j.ejcb.2019.151044.

References

Albuschies, J., Vogel, V., 2013. The role of filopodia in the recognition of nanotopographies. Sci. Rep. 3, 1658. https://doi.org/10.1038/srep01658.

Almagro, S., Durmort, C., Chervin-Pétinot, A., Heyraud, S., Dubois, M., Lambert, O., Maillefaud, C., Hewat, E., Schaal, J.P., Huber, P., Gulino-Debrac, D., 2010. The motor protein myosin-X transports VE-cadherin along filopodia to allow the formation of early endothelial cell-cell contacts. Mol. Cell. Biol. 30, 1703–1717. https://doi.org/

10.1128/MCB.01226-09.
Amieva, M.R., Furthmayr, H., 1995. Subcellular localization of moesin in dynamic filopodia, retraction fibers, and other structures involved in substrate exploration, attachment, and cell-cell contacts. Exp. Cell Res. 219, 180–196. https://doi.org/10.1006/excr.1995.1218.
Arjonen, A., Kaukonen, R., Ivaska, J., 2011. Filopodia and adhesion in cancer cell motility. Cell Adh. Migr. 5, 421–430. https://doi.org/10.4161/cam.5.5.17723.
Bandeira, C.L., Urban Borbely, A., Pulcineli Vieira Francisco, R., Schultz, R., Zugaib, M., Bevilacqua, E., 2014. Tumorigenic factor CRIPTO-1 is immunolocalized in extravillous cytotrophoblast in placenta creta. Biomed. Res. Int. 2014, 1–9. https://doi.org/10.1155/2014/892856.
Beck, S., Le Good, J.A., Guzman, M., Haim, N.Ben, Roy, K., Beermann, F., Constam, D.B., 2002. Extraembryonic proteases regulate Nodal signalling during gastrulation. Nat. Cell Biol. 4, 981–985. https://doi.org/10.1038/ncb890.
Bianco, C., Rangel, M.C., Castro, N.P., Nagaoka, T., Rollman, K., Gonzales, M., Salomon, D.S., 2010. Role of Cripto-1 in stem cell maintenance and malignant progression. Am. J. Pathol. 177, 532–540. https://doi.org/10.2353/ajpath.2010.100102.
Chu, J., Ding, J., Jeays-Ward, K., Price, S.M., Placzek, M., Shen, M.M., 2005. Non-cell-autonomous role for Cripto in axial midline formation during vertebrate embryogenesis. Development 132, 5539–5551. https://doi.org/10.1242/dev.02157.
Cramer, L.P., Mitchison, T.J., 1997. Investigation of the mechanism of retraction of the cell margin and rearward flow of nodules during mitotic cell rounding. Mol. Biol. Cell 8, 109–119.
Ding, J., Yang, L., Yan, Y.-T., Chen, A., Desai, N., Wynshaw-Boris, A., Shen, M.M., 1998. Cripto is required for correct orientation of the anterior–posterior axis in the mouse embryo. Nature 395, 702–707. https://doi.org/10.1038/27215.
Fairchild, C.L., Barna, M., 2014. Specialized filopodia: at the "tip" of morphogen transport and vertebrate tissue patterning. Curr. Opin. Genet. Dev. 27, 67–73. https://doi.org/10.1016/j.gde.2014.03.013.
Fantin, A., Lampropoulou, A., Gestri, G., Raimondi, C., Senatore, V., Zachary, I., Ruhrberg, C., 2015. NRP1 regulates CDC42 activation to promote filopodia formation in endothelial tip cells. Cell Rep. 11, 1577–1590. https://doi.org/10.1016/j.celrep.2015.05.018.
Francescangeli, F., Contavalli, P., De Angelis, M.L., Baiocchi, M., Gambara, G., Pagliuca, a, Fiorenzano, a, Prezioso, C., Boe, a, Todaro, M., Stassi, G., Castro, N.P., Watanabe, K., Salomon, D.S., De Maria, R., Minchiotti, G., Zeuner, a, 2015. Dynamic regulation of the cancer stem cell compartment by Cripto-1 in colorectal cancer. Cell Death Differ. 1–14. https://doi.org/10.1038/cdd.2015.19.
Gudbergsson, J.M., Kostrikov, S., Johnsen, K.B., Fliedner, F.P., Stolberg, C.B., Humle, N., Hansen, A.E., Kristensen, B.W., Christiansen, G., Kjær, A., Andresen, T.L., Duroux, M., 2019. A tumorsphere model of glioblastoma multiforme with intratumoral heterogeneity for quantitative analysis of cellular migration and drug response. Exp. Cell Res. 379, 73–82. https://doi.org/10.1016/J.YEXCR.2019.03.031.
Härkönen, K., Oikari, S., Kyykallio, H., Capra, J., Hakkola, S., Ketola, K., Thanigai Arasu, U., Daaboul, G., Malloy, A., Oliveira, C., Jokelainen, O., Sironen, R., Hartikainen, J.M., Rilla, K., Härkönen, K., Oikari, S., Kyykallio, H., Capra, J., Hakkola, S., Ketola, K., Thanigai Arasu, U., Daaboul, G., Malloy, A., Oliveira, C., Jokelainen, O., Sironen, R., Hartikainen, J.M., Rilla, K., 2019. CD44s assembles hyaluronan coat on filopodia and extracellular vesicles and induces tumorigenicity of MKN74 gastric carcinoma cells. Cells 8, 276. https://doi.org/10.3390/cells8030276.
He, K., Sakai, T., Tsukasaki, Y., Watanabe, T.M., Ikebe, M., 2017. Myosin X is recruited to nascent focal adhesions at the leading edge and induces multi-cycle filopodial elongation. Sci. Rep. 7, 13685. https://doi.org/10.1038/s41598-017-06147-6.
Huang, C., Chen, W., Wang, X., Zhao, J., Li, Q., Fu, Z., 2015. Cripto-1 promotes the epithelial-mesenchymal transition in esophageal squamous cell carcinoma cells. Evid. Complement. Alternat. Med. 2015, 1–13. https://doi.org/10.1155/2015/421285.
Jacquemet, G., Hamidi, H., Ivaska, J., 2015. Filopodia in cell adhesion, 3D migration and cancer cell invasion. Curr. Opin. Cell Biol. 36, 23–31. https://doi.org/10.1016/j.ceb.2015.06.007.
Jain, A., Mallupattu, S., Thakur, R., Ghoshal, S., Pal, A., 2018. Cripto 1, a potential biomarker for oral squamous cell carcinoma. Oral Oncol. https://doi.org/10.1016/j.oraloncology.2018.11.001.
Klauzinska, M., Castro, N.P., Rangel, M.C., Spike, B.T., Gray, P.C., Bertolette, D., Cuttitta, F., Salomon, D., 2014. The multifaceted role of the embryonic gene Cripto-1 in cancer, stem cells and epithelial-mesenchymal transition. Semin. Cancer Biol. 29, 1–8. https://doi.org/10.1016/j.semcancer.2014.08.003.
Liu, Q., Cui, X., Yu, X., Bian, B.-S.-J., Qian, F., Hu, X., Ji, C., Yang, L., Ren, Y., Cui, W., Zhang, X., Zhang, P., Wang, J.M., Cui, Y., Bian, X., 2017a. Cripto-1 acts as a functional marker of cancer stem-like cells and predicts prognosis of the patients in esophageal squamous cell carcinoma. Mol. Cancer 16, 81. https://doi.org/10.1186/s12943-017-0650-7.
Liu, Y., Qin, Z., Yang, K., Liu, R., Xu, Y., 2017b. Cripto-1 promotes epithelial-mesenchymal transition in prostate cancer via Wnt/β-catenin signaling. Oncol. Rep. 37, 1521–1528. https://doi.org/10.3892/or.2017.5378.
Lo, R.C.-L., Leung, C.O.-N., Chan, K.K.-S., Ho, D.W.-H., Wong, C.-M., Lee, T.K.-W., Ng, I.O.-L., 2018. Cripto-1 contributes to stemness in hepatocellular carcinoma by stabilizing Dishevelled-3 and activating Wnt/β-catenin pathway. Cell Death Differ. https://doi.org/10.1038/s41418-018-0059-x.
Luz, M., Spannl-Müller, S., Özhan, G., Kagermeier-Schenk, B., Rhinn, M., Weidinger, G., Brand, M., 2014. Dynamic association with donor cell filopodia and lipid-modification are essential features of Wnt8a during patterning of the zebrafish neuroectoderm. PLoS One 9, e84922. https://doi.org/10.1371/journal.pone.0084922.
Ma, L., Li, Y., Peng, J., Wu, D., Zhao, X., Cui, Y., Chen, L., Yan, X., Du, Y., Yu, L., 2015. Discovery of the migrasome, an organelle mediating release of cytoplasmic contents during cell migration. Cell Res. 25, 24–38. https://doi.org/10.1038/cr.2014.135.
Machesky, L.M., 2008. Lamellipodia and filopodia in metastasis and invasion. FEBS Lett. 582, 2102–2111. https://doi.org/10.1016/J.FEBSLET.2008.03.039.
Mattes, B., Dang, Y., Greicius, G., Kaufmann, L.T., Prunsche, B., Rosenbauer, J., Stegmaier, J., Mikut, R., Özbek, S., Nienhaus, G.U., Schug, A., Virshup, D.M., Scholpp, S., 2018. Wnt/PCP controls spreading of Wnt/β-catenin signals by cytonemes in vertebrates. Elife 7. https://doi.org/10.7554/eLife.36953.
Mayer, C., Maaser, K., Daryab, N., Zänker, K.S., Bröcker, E.B., Friedl, P., 2004. Release of cell fragments by invading melanoma cells. Eur. J. Cell Biol. 83, 709–715. https://doi.org/10.1078/0171-9335-00394.
Memmel, S., Sukhorukov, V.L., Höring, M., Westerling, K., Fiedler, V., Katzer, A., Krohne, G., Flentje, M., Djuzenova, C.S., 2014. Cell surface area and membrane folding in glioblastoma cell lines differing in PTEN and p53 status. PLoS One 9, e87052. https://doi.org/10.1371/journal.pone.0087052.
Mitchison, T.J., 1992. Actin based motility on retraction fibers in mitotic PtK2 cells. Cell Motil. Cytoskeleton 22, 135–151. https://doi.org/10.1002/cm.970220207.
Moti, N., Yu, J., Boncompain, G., Perez, F., Virshup, D.M., 2019. Wnt traffic from endoplasmic reticulum to filopodia. PLoS One 14, e0212711. https://doi.org/10.1371/journal.pone.0212711.
Normanno, N., De Luca, A., Bianco, C., Maiello, M.R., Carriero, M.V., Rehman, A., Wechselberger, C., Arra, C., Strizzi, L., Sanicola, M., Salomon, D.S., 2004. Cripto-1 overexpression leads to enhanced invasiveness and resistance to anoikis in human MCF-7 breast cancer cells. J. Cell. Physiol. 198, 31–39. https://doi.org/10.1002/jcp.10375.
Patla, I., Volberg, T., Elad, N., Hirschfeld-Warneken, V., Grashoff, C., Fässler, R., Spatz, J.P., Geiger, B., Medalia, O., 2010. Dissecting the molecular architecture of integrin adhesion sites by cryo-electron tomography. Nat. Cell Biol. 12, 909–915. https://doi.org/10.1038/ncb2095.
Pilgaard, L., Mortensen, J.H., Henriksen, M., Olesen, P., Sørensen, P., Laursen, R., Vyberg, M., Agger, R., Zachar, V., Moos, T., Duroux, M., 2014. Cripto-1 expression in glioblastoma multiforme. Brain Pathol. 24, 360–370. https://doi.org/10.1111/bpa.12131.
Porter, K.R., Claude, A., Fullam, E.F., 1945. A study of tissue culture cells by electron microscopy: methods and preliminary observations. J. Exp. Med. 81, 233–246.
Rasmussen, R.D., Gajjar, M.K., Tuckova, L., Jensen, K.E., Maya-Mendoza, A., Holst, C.B., Møllgaard, K., Rasmussen, J.S., Brennum, J., Bartek, J., Syrucek, M., Sedlakova, E., Andersen, K.K., Frederiksen, M.H., Bartek, J., Hamerlik, P., 2016. BRCA1-regulated RRM2 expression protects glioblastoma cells from endogenous replication stress and promotes tumorigenicity. Nat. Commun. 7, 13398. https://doi.org/10.1038/ncomms13398.
Ravisankar, V., Singh, T.P., Manoj, N., 2011. Molecular evolution of the EGF–CFC protein family. Gene 482, 43–50. https://doi.org/10.1016/j.gene.2011.05.007.
Sagar, Pröls, F., Wiegreffe, C., Scaal, M., 2015. Communication between distant epithelial cells by filopodia-like protrusions during embryonic development. Development 142, 665–671. https://doi.org/10.1242/dev.115964.
Sanders, T.A., Llagostera, E., Barna, M., 2013. Specialized filopodia direct long-range transport of SHH during vertebrate tissue patterning. Nature 497, 628–632. https://doi.org/10.1038/nature12157.
Schindelin, J., Arganda-Carreras, I., Frise, E., Kaynig, V., Longair, M., Pietzsch, T., Preibisch, S., Rueden, C., Saalfeld, S., Schmid, B., Tinevez, J.-Y., White, D.J., Hartenstein, V., Eliceiri, K., Tomancak, P., Cardona, A., 2012. Fiji: an open-source platform for biological-image analysis. Nat. Methods 9, 676–682. https://doi.org/10.1038/nmeth.2019.
Stanganello, E., Hagemann, A.I.H., Mattes, B., Sinner, C., Meyen, D., Weber, S., Schug, A., Raz, E., Scholpp, S., 2015. Filopodia-based Wnt transport during vertebrate tissue patterning. Nat. Commun. 6, 5846. https://doi.org/10.1038/ncomms6846.
Steketee, M.B., Tosney, K.W., 2002. Three functionally distinct adhesions in filopodia: shaft adhesions control lamellar extension. J. Neurosci. 22, 8071–8083.
Strizzi, L., Bianco, C., Normanno, N., Salomon, D., 2005. Cripto-1: a multifunctional modulator during embryogenesis and oncogenesis. Oncogene 24, 5731–5741. https://doi.org/10.1038/sj.onc.1208918.
Strizzi, L., Bianco, C., Normanno, N., Seno, M., Wechselberger, C., Wallace-Jones, B., Khan, N.I., Hirota, M., Sun, Y., Sanicola, M., Salomon, D.S., 2004. Epithelial mesenchymal transition is a characteristic of hyperplasias and tumors in mammary gland from MMTV-Cripto-1 transgenic mice. J. Cell. Physiol. 201, 266–276. https://doi.org/10.1002/jcp.20062.
Strizzi, L., Margaryan, N.V., Gilgur, A., Hardy, K.M., Normanno, N., Salomon, D.S., Hendrix, M.J.C., 2013. The significance of a Cripto-1 positive subpopulation of human melanoma cells exhibiting stem cell-like characteristics. Cell Cycle 12, 1450–1456. https://doi.org/10.4161/cc.24601.
Svitkina, T.M., Bulanova, E.A., Chaga, O.Y., Vignjevic, D.M., Kojima, S., Vasiliev, J.M., Borisy, G.G., 2003. Mechanism of filopodia initiation by reorganization of a dendritic network. J. Cell Biol. 160, 409–421. https://doi.org/10.1083/jcb.200210174.
Taylor, A.C., Robbins, E., 1963. Observations on microextensions from the surface of isolated vertebrate cells. Dev. Biol. 7, 660–673. https://doi.org/10.1016/0012-1606(63)90150-7.
Tysnes, B.B., Sætran, H.A., Mørk, S.J., Margaryan, N.V., Eide, G.E., Petersen, K., Strizzi, L., Hendrix, M.J.C., 2013. Age-dependent association between protein expression of the embryonic stem cell marker cripto-1 and survival of glioblastoma patients. Transl. Oncol. 6https://doi.org/10.1593/tlo.13427. 732-IN33.
Virgintino, D., Rizzi, M., Errede, M., Strippoli, M., Girolamo, F., Bertossi, M., Roncali, L., 2012. Plasma membrane-derived microvesicles released from tip endothelial cells during vascular sprouting. Angiogenesis 15, 761–769. https://doi.org/10.1007/s10456-012-9292-y.
Warner, D.R., Greene, R.M., Pisano, M.M., 2005. Cross-talk between the TGFβ and Wnt signaling pathways in murine embryonic maxillary mesenchymal cells. FEBS Lett. 579, 3539–3546. https://doi.org/10.1016/j.febslet.2005.05.024.
Watanabe, K., Bianco, C., Strizzi, L., Hamada, S., Mancino, M., Bailly, V., Mo, W., Wen, D.,

Miatkowski, K., Gonzales, M., Sanicola, M., Seno, M., Salomon, D.S., 2007. Growth factor induction of Cripto-1 shedding by glycosylphosphatidylinositol-phospholipase D and enhancement of endothelial cell migration. J. Biol. Chem. 282, 31643–31655. https://doi.org/10.1074/jbc.M702713200.

Watanabe, K., Salomon, D.S., 2010. Intercellular transfer regulation of the paracrine activity of GPI-anchored Cripto-1 as a Nodal co-receptor. Biochem. Biophys. Res. Commun. 403, 108–113. https://doi.org/10.1016/j.bbrc.2010.10.128.

Watanabe, T.M., Tokuo, H., Gonda, K., Higuchi, H., Ikebe, M., 2010. Myosin-X induces filopodia by multiple elongation mechanism. J. Biol. Chem. 285, 19605–19614. https://doi.org/10.1074/jbc.M109.093864.

Wei, B., Jin, W., Ruan, J., Xu, Z., 2015. Cripto-1 expression and its prognostic value in human bladder cancer patients. J. Immunother. Emphasis Tumor Immunol. 1105–1113. https://doi.org/10.1007/s13277-014-2695-1.

Xu, C.H., Wang, Y., Qian, L.H., Yu, L.K., Zhang, X.W., Wang, Q.B., 2017. Serum Cripto-1 is a novel biomarker for non-small cell lung cancer diagnosis and prognosis. Clin. Respir. J. 11, 765–771. https://doi.org/10.1111/crj.12414.

Yang, C., Svitkina, T., 2011. Filopodia initiation: focus on the Arp2/3 complex and formins. Cell Adh. Migr. 5, 402–408. https://doi.org/10.4161/cam.5.5.16971.

Zhang, H., Berg, J.S., Li, Z., Wang, Y., Lång, P., Sousa, A.D., Bhaskar, A., Cheney, R.E., Strömblad, S., 2004. Myosin-X provides a motor-based link between integrins and the cytoskeleton. Nat. Cell Biol. 6, 523–531. https://doi.org/10.1038/ncb1136.

Zhang, Y., Xu, H., Chi, X., Fan, Y., Shi, Y., Niu, J., 2018. High level of serum Cripto-1 in hepatocellular carcinoma, especially with hepatitis B virus infection. Medicine (Baltimore) 97, e11781. https://doi.org/10.1097/MD.0000000000011781.